Computers and Mathematics with Applications 58 (2009) 1015–1023

Contents lists available at ScienceDirect

Computers and Mathematics with Applications

journal homepage: www.elsevier.com/locate/camwa

Regional scale transient groundwater flow modeling using Lattice Boltzmann methods

Shadab Anwar *, Michael C. Sukop

Earth Sciences, Florida International University, University Park, Miami, FL 33199, USA

ARTICLE INFO

Keywords:
Porous media
Theis solution
Lattice Boltzmann
Ground water

ABSTRACT

Lattice Boltzmann (LB) models can be used to simulate flow in porous media at scales much larger than pore size. LB-based models for such macroscopic scale porous media flow simulations are an extension of standard LB models. There are at least two alternative approaches for implementing such models. In the first approach the local velocity is altered during the collision step by incorporating an external force, **F**, equivalent to the damping effect of solid particles in porous media. The porous media can be permeable or impermeable depending upon the external forcing term. A sink term is introduced in the LB model to simulate a pumping well and this model is further applied to solve transient ground water well problems for confined aquifers.

Directly solving the ground water flow equation with an LB model by exploiting its ability to solve the diffusion equation is another strategy. The second order transient ground water flow equation is analogous to the diffusion equation and mass diffusivity is analogous to hydraulic diffusivity. This diffusion model is used to solve transient ground water problems. Simulated results accurately match analytical solutions of the transient ground water flow equation.

1. Introduction

Simulation of flow in large scale porous media (e.g., an 'aquifer' in hydrology) by solving the Navier–Stokes equations (NSE) at pore scale is computationally prohibitive. A common method employed to solve such problems is to use representative properties, which consider the overall effect of the porous medium on the flow. The Representative Elementary Volume (REV) is a scale above which microscopic heterogeneity can be ignored and the medium can be assumed uniform or homogeneous [1]. Darcy's law is used to compute the volumetric flux (q (m/s)) of fluid flowing under a constant head (h) or pressure (p) gradient across a porous medium of (possibly tensorial) permeability, k (m^2):

$$\mathbf{q} = -\frac{kg}{\nu}\nabla h, \tag{1}$$

where g ($\mathrm{m/s}^2$) is the acceleration due to gravity and ν (m^2/s) is the kinematic viscosity of fluid. We use Darcy's law in terms of head gradient because this is traditional in hydrology. Boundary conditions and solutions of ground water problems are generally defined in terms of head and not pressure. Darcy's law is applicable only for the Stokes flow regime on the REV scale and above, and gives an averaged macroscopic flux for a porous medium. Following application of the conservation of mass (or volume for incompressible flow) to a porous medium above the REV, Darcy's law is the constitutive equation

* Corresponding author.
E-mail addresses: sanwa001@fiu.edu (S. Anwar), sukopm@fiu.edu (M.C. Sukop).

0898-1221/$ – see front matter © 2009 Elsevier Ltd. All rights reserved.
doi:10.1016/j.camwa.2009.02.025

used to derive the transient groundwater flow equation, which is completely analogous to the well-known heat equation (e.g., [2]) and is given below with (Eq. (2)) and without (Eq. (3)) a sink term.

The motivation for this work is to establish LBM as an alternative and improved technique for modeling transient groundwater hydraulics problems. LBM is particularly useful and holds great promise for fractured porous media or karst aquifers (limestone with caves and other conduits). Fluid flow must be solved using different approaches in conduits (NSE) and the surrounding porous media (Darcy's law-based ground water flow equation). LBM may not be superior to traditional methods for simple confined aquifer problems presented in this paper, but our results lay groundwork for the development of LB models for large scale, complex problems such as karst aquifers for example.

1.1. Transient groundwater flow equations

In the absence of source/sink terms, groundwater head distribution follows the transient ground water flow equation as shown below:

$$\frac{\partial h}{\partial t} = \frac{T}{S}\nabla^2 h. \tag{2}$$

h is the head of water at any time (t) in an aquifer of transmissivity (T) and storage coefficient (S). The transmissivity of an aquifer represents the volumetric flow rate (Q) per unit width of an aquifer (W) under a unit hydraulic gradient (∇h). The storage coefficient, S indicates the volume of yield per unit change in head per unit surface area of aquifer. This is a non-dimensional parameter.

The transient groundwater flow equation for a domain with a pumping well (i.e., a source or sink) in a confined aquifer is [3]:

$$\frac{\partial h}{\partial t} = \frac{T}{S}\nabla^2 h + \frac{q}{S}. \tag{3}$$

These two equations have very important differences. In Eq. (2), only the ratio of hydraulic diffusivity (T/S) is important and the effects of the two hydraulic parameters cannot be separated. The presence of source/sink term in Eq. (3) allows distinct contributions from the hydraulic parameters, S and T.

This paper is organized as follows: standard Bhatnagar–Gross–Krook (BGK) LB methods are reviewed and two types of LB models for flow simulation in macroscopic porous media are introduced in Section 2. In Section 3, a transient ground water flow problem is solved using both the LB models and results are shown. In Section 4, a transient groundwater flow equation with a pumping well is solved with an LB model. In Section 5, conclusions are presented.

2. LBM

2.1. BGK model

Lattice Boltzmann models have been successfully applied to simulate fluid flow in complicated geometries such as those presented by porous media [4–6]. It has been proven that the NSE can be derived from the Boltzmann equation in the low Mach number limit [7]. The LB model solves for the particle distribution function in the linearized Boltzmann equation on discrete lattices at mesoscopic scale. The particle distribution function (f) defines the occurrence of a hypothetical group of particles with momentum ($\mathbf{p}$) at any location ($\mathbf{x}$) and time (t). At each time step, f updates through a collision mechanism and streams (propagates) to the nearest neighboring node in discrete directions j with discrete microscopic velocity ($\mathbf{e}_j$). The macroscopic properties such as density (ρ)

$$\rho = \sum_{j=0}^{8} f_j \tag{4}$$

and velocity ($\mathbf{u}$)

$$\mathbf{u} = \frac{1}{\rho}\sum_{j=0}^{8} f_j \mathbf{e}_j, \tag{5}$$

conform to the continuity equation

$$\frac{\partial \rho}{\partial t} + \nabla \cdot \rho\mathbf{u} = 0 \tag{6}$$

and momentum equation at Navier–Stokes scale:

$$\frac{\partial (\rho\mathbf{u})}{\partial t} + \nabla[\rho\mathbf{u}\mathbf{u}] = -\nabla p + \nabla[\rho\nu(\nabla\mathbf{u} + \mathbf{u}\nabla)]. \tag{7}$$

$p = \frac{1}{3}\rho$ is the fluid pressure. The time evolution of f follows the equation

$$f_j(\mathbf{x} + \mathbf{e}_j\delta t, t + \delta t) = f_j(\mathbf{x}, t) - \delta t \left(\frac{f_j(\mathbf{x}, t) - f_j^{eq}(\mathbf{x}, t)}{\tau} \right), \tag{8}$$

where incrementing the spatial subscripts by $e_j\delta t$ in $f_j(\mathbf{x} + \mathbf{e}_j\delta t, t + \delta t)$ is the streaming part and $\delta t \left(\frac{f_j(\mathbf{x},t) - f_j^{eq}(\mathbf{x},t)}{\tau} \right)$ is the collision term representing the rate of change of the particle distribution function due to collision. The collision operator is simplified in the BGK model by use of a single relaxation time τ for all directions. τ is a relaxation time that indicates the rate at which the system approaches equilibrium through collision. The equilibrium distribution function f^{eq} for the 2-dimensional, 9 velocity model ($D2Q9$) is [7]

$$f_j^{eq}(\mathbf{x}) = t_j^* \rho(\mathbf{x}) \left(c_s^2 + \mathbf{e}_j \cdot \mathbf{u} + \frac{3}{2}(\mathbf{e}_j \cdot \mathbf{u})^2 - \frac{1}{2}\mathbf{u}^2 \right). \tag{9}$$

The weights (t_j^*) are $\frac{1}{3}$ for $j = 1, 2, 3, 4$ (main Cartesian axes), and $\frac{1}{12}$ for $j = 5, 6, 7, 8$ (diagonals). The weight for $j = 0$ rest particles is $t_0 = 1 - c_s^2 \sum t_j = 1 - \frac{5}{3}c_s^2 = \frac{4}{9}$ [8]. The domain is discretized into a square lattice space with lattice spacing $\Delta x = 1$. $c_s^2 = \frac{1}{3}c^2$ where, c_s is speed of sound and $c = \frac{\Delta x}{\Delta t} = 1$ [9]. LBM boundary conditions applied here follow the approach of [25].

Two different approaches are available for the solution of the transient ground water flow equations (2) and (3), with LBM. The first approach, which is based on the incorporation of a resistance term and a related alteration of the velocity, has been applied to the simulation of steady state flows in porous media for over 10 years, but not previously to transient problems. The second exploits the LBM's ability to solve the heat equation directly and has only recently been applied elsewhere (e.g., [10]).

2.2. Altered-velocity model

Various LB methods have been proposed to transform the normal Navier–Stokes LBM solver into a Darcy's law solver that can be applied at any scale [11–15]. The nodes in a porous media model represent a volume of a porous medium, which contains numerous pores and solids [13]. The most common approach is to introduce an external force by dynamically changing the local velocity during the collision step [11]. This approach is closely related to the inclusion of interphase force or gravity forces in LB models [16,17].

Solid particles in a porous medium offer resistance to flow and interconnectivity of the pores facilitates flow through the porous medium. The resistance field $\mathbf{R}^*$ can be related to the pressure drop across a porous medium. This resistance field could be a tensor to take into account the direction-dependent permeability of any particular porous medium. Eq. (1) can be written in terms of a resistance field $\mathbf{R}^*$ [13] and pressure p:

$$\nabla p = -\rho \mathbf{R}^* q. \tag{10}$$

This model treats the porous medium as a resistance field and calculates the volumetric flux (q) for a given pressure gradient, ∇p. Freed [13] defined this approach as an averaging of the steady state NSE over the local sub-volume in the Stokes regime where viscous forces are replaced by the resistive force as shown on the RHS of Eq. (10). Some new notation [13] is introduced to define the change in macroscopic velocity: $\tilde{\mathbf{u}}$ is the pre-collision velocity, $\mathbf{u}'$ is the post-collision velocity and $\bar{\mathbf{u}}$ is the mean centered velocity. An external force $\mathbf{F}$ is

$$\mathbf{F} = \frac{\rho}{\tau} \left(\mathbf{u}' - \tilde{\mathbf{u}} \right) \tag{11}$$

which is equivalent to the term $\rho \mathbf{R}^* \cdot \mathbf{u}$:

$$\frac{\rho}{\tau} \left(\mathbf{u}' - \tilde{\mathbf{u}} \right) = \rho \mathbf{R}^* \cdot \mathbf{u}. \tag{12}$$

The resistance field is related to the permeability as

$$\mathbf{R}^* = \nu \mathbf{k}^{-1}. \tag{13}$$

Mean centered velocity ($\bar{\mathbf{u}}$) should be used as the actual macroscopic velocity, and is calculated as

$$\bar{\mathbf{u}} = \left[1 - \frac{1}{2\tau} \right] \tilde{\mathbf{u}} + \frac{1}{2\tau} \mathbf{u}' \tag{14}$$

where

$$\mathbf{u}' = \mathbf{G} \cdot \tilde{\mathbf{u}} \tag{15}$$

and

$$\mathbf{G} = \frac{1 - [\tau - \frac{1}{2}]\mathbf{R}^*}{1 + \frac{1}{2}\mathbf{R}^*}. \tag{16}$$

The algorithm for the porous media model is

$$f_j(\mathbf{x} + \mathbf{e}_j\delta t, t + \delta t) = f_j(\mathbf{x}, t) - \delta t \left(\frac{f_j(\mathbf{x}, t) - f_j^{eq}(\mathbf{x}, t)}{\tau} \right), \tag{17}$$

and

$$f_j^{eq}(\mathbf{x}) = t_j^* \rho(\mathbf{x}) \left(c_s^2 + \mathbf{e}_j \cdot \mathbf{u}' + \frac{3}{2}(\mathbf{e}_j \cdot \mathbf{u}')^2 - \frac{1}{2}\overline{\mathbf{u}}^2 \right), \tag{18}$$

where, $\overline{\mathbf{u}}$ and $\mathbf{u}'$ are given by Eqs. (14) and (15). The resulting macroscopic hydrodynamics will be governed by Eq. (6) and the modified momentum equation, which at the Navier–Stokes scale is [13]:

$$\frac{\partial \rho \overline{\mathbf{u}}}{\partial t} + \nabla \cdot [\rho \overline{\mathbf{u}}\overline{\mathbf{u}}] = -\nabla p - \rho \mathbf{R}^* \cdot \overline{\mathbf{u}} + \nabla[\rho\nu(\nabla\overline{\mathbf{u}} + \overline{\mathbf{u}}\nabla)]. \tag{19}$$

$\overline{\mathbf{u}}$ is equal to the macroscopic Darcy flux (q).

The LHS of Eq. (19) represents the total acceleration of moving fluid: time-dependent acceleration and space-dependent convective acceleration. These accelerations become zero for creeping flow. The last term on the RHS accounts for the Brinkman correction and it becomes negligible for creeping flow in porous media [15]. The only terms left behind are first two terms on the RHS which are same as Eq. (10). Eq. (10) can easily be written as Eq. (1) using Eq. (13).

The regular LB model (Eqs. (8) and (9)) solves the NSE. Hence the $f_j^{eq}(\mathbf{x})$ is modified to include a resistance term so that LBM solves the modified NSE represented by Eq. (19). Eq. (19) solves both the NSE or the macroscopic flow field, which is also given by Eq. (1), depending upon the value of $\mathbf{R}^*$. If the $\mathbf{R}^*$ value is zero, the node does not cause any resistance to flow and the Eq. (19) solves the NSE; when $\mathbf{R}^*$ has a non-zero value, Eq. (19) solves the Darcy equation with permeability at a node given by Eq. (13). No explicit switch is necessary to switch between the NSE and Darcy equations.

Eq. (19) is not directly linked with Eqs. (2) and (3). The density calculated with (4) using the modified f^{eq} of (18) is used as head. This LB-based, altered-velocity flow model has been verified against Darcy's law under Stokes regime flow and against analytical solutions for flow between parallel plates with and without a homogeneous porous medium between them [13,14,12,15]. These are steady state solutions of flow, and the inflow of mass (volume for incompressible flow) is strictly equal to outflow. In this paper, two different kinds of LB models are applied to solve transient ground water flow equations that involve changes in fluid storage.

2.3. LB-based diffusion model

In Eq. (2), the coefficient on the RHS represents the hydraulic diffusivity of the aquifer, analogous to the coefficient of molecular diffusion in the diffusion equation and the thermal diffusivity in the heat equation. As noted by Ginzburg [8], the LB-based diffusion model represents another strategy for solving the transient ground water flow equation, in addition to the altered-velocity flow model described above. Recently Serván Camas [10] solved the Henry problem [18] using an LB-based diffusion model.

Flekkøy [19] introduced an LB model to simulate diffusion and miscible fluid flow in 2D and 3D. A separate equilibrium distribution function with its own relaxation parameter is used to simulate the advection–diffusion equation. Equilibrium distribution functions for flow and transport are coupled through a common macroscopic flow velocity; hence the solute component B behaves as a passive scalar. The equilibrium distribution function for component B is a truncated form of Eq. (9). It has only first order velocity terms:

$$f_{Bj}^{eq}(\mathbf{x}) = t_j^* \rho_B(\mathbf{x})[c_s^2 + \mathbf{e}_j \cdot \mathbf{u}_A]. \tag{20}$$

The density (concentration) for component B is computed following Eq. (4) and its velocity $\mathbf{u}_A$ is assigned from component A; B is advected along with A as a passive scalar. The mass diffusivity D_m between two species is expressed in terms of relaxation time τ_B for component B [19]:

$$D_m = c_s^2\left[\tau_B - \frac{1}{2}\right]. \tag{21}$$

This has been successfully used to solve diffusion/dispersion problems under various initial and boundary conditions [20]. The diffusion coefficient controls the mixing of tracer with background fluid. Similarly, hydraulic diffusivity ($D = T/S$) for an aquifer controls the change in head across the aquifer over time. The analogy between the diffusion equation and the transient flow equation can be used to solve head distribution over the aquifer using the lattice Boltzmann model for the diffusion problem by setting $u_A = 0$ in Eq. (20) and equating the head with the density of component B.

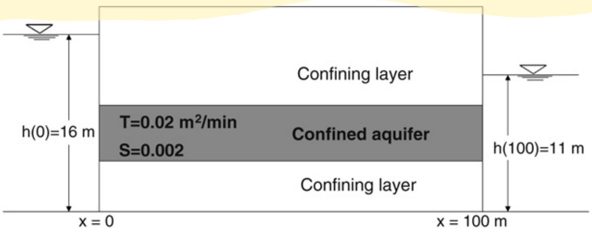

Fig. 1. Schematic representation of aquifer.

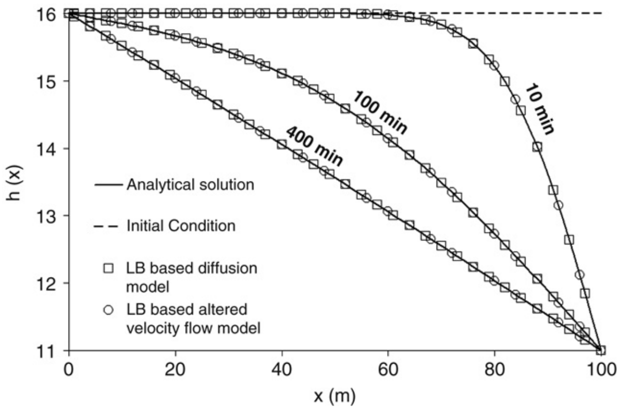

Fig. 2. Transient change in head as a response to a sudden change in head at right boundary for two different solutions techniques vs. analytical results.

3. Transient ground water flow problem without source/sink

Wang and Anderson [3] present a transient groundwater flow problem in which an aquifer responds to a sudden change in one of the boundary conditions. The aquifer is assumed one-dimensional and is confined by impermeable layers on top and bottom as shown in Fig. 1. In this case, there is no source/sink and the transient ground water flow equation (2) becomes in 1-D

$$\frac{\partial h}{\partial t} = \frac{T}{S}\frac{\partial^2 h}{\partial x^2}. \tag{22}$$

The aquifer is connected by reservoirs at $x = 0$ and $x = 100$ m. Initially the aquifer has uniform head equal to 16 m. The aquifer parameters are $T = 0.02$ m^2/ min and $S = 0.002$; at $t = 0+$ the reservoir boundary on the RHS instantly falls to $h = 11$ m. The aquifer responds to this sudden change in head by ultimately reaching a steady state linear head distribution between the reservoirs.

Since the transient ground water equation as shown in Eq. (2) is analogous to the diffusion equation, we can use the idea of diffusion length to relate the real time with the lattice time step (ts). For L_D a characteristic length, diffusion coefficient D, and time t:

$$\xi = \frac{Dt}{{L_D}^2}, \tag{23}$$

is a non-dimensional number, which will be identical in real physical units and LB units.

3.1. LB-based diffusion model

First we solve the transient reservoir problem of Fig. 1 with the LB-based diffusion model. To achieve the same ξ value, we use the LB model of domain size 100 lu × 10 lu and the model parameters are $\tau_B = 0.8$ ts, which leads to $D = 0.1$ lu^2/ts. The diffusivity in the LB model is reduced by 100 times and time step is increased by 100 times compared to the real values to keep ξ the same as in the physical problem at each simulated time (Table 1).

The results are plotted in Fig. 2 for 1000 ts (10 min), 10 000 ts (100 min) and 40 000 ts (400 min). This demonstrates that we can solve transient groundwater head distribution using an LB-based diffusion model. Without a source/sink, the only parameter we can change in this model is hydraulic diffusivity via the relaxation time τ_B. Thus, it is not possible to simulate groundwater problems governed by Eq. (3) and characterized by the potential for independent variation of S and T with this model in its current form; source/sink terms would have to be added to the LB model.

Table 1
Parameters in real and lattice units as used in LB-based diffusion model.

T_{real} $\left(\frac{\text{m}^2}{\text{min}}\right)$	S_{real} (–)	D_{real} $\left(\frac{\text{m}^2}{\text{min}}\right)$	t_{real} (min)	$(L_D)_{\text{real}}$ (m)	ξ (–)	$(L_D)_{\text{LBM}}$ (lu)	D_{LBM} $\left(\frac{\text{lu}^2}{\text{ts}}\right)$	τ_B (-)	t_{LBM} (ts)
0.02	.002	10	10	100	0.01	100	0.1	0.8	1 000
0.02	.002	10	100	100	0.1	100	0.1	0.8	10 000
0.02	.002	10	400	100	0.4	100	0.1	0.8	40 000

Table 2
Parameters used in altered-velocity model.

t_{real} (min)	τ_B (ts)	$\mathbf{R}^*$ (–)	T_{LBM} $\left(\frac{\text{lu}^2}{\text{ts}}\right)$	S_{LBM} (–)	D_{LBM} $\left(\frac{\text{lu}^2}{\text{ts}}\right)$	ξ (–)	L_D (lu)	t_{LBM} (ts)
10	0.96	1	0.32	0.96	$\frac{1}{3}$	0.01	100	300
100	0.96	1	0.32	0.96	$\frac{1}{3}$	0.1	100	3 000
400	0.96	1	0.32	0.96	$\frac{1}{3}$	0.4	100	12 000

3.2. Altered-velocity flow model

It is also possible to solve transient groundwater flow problems using the LB-based altered-velocity flow model. We simulate the same boundary value problem as shown above in Fig. 1 using the altered-velocity flow model here.

First we need to resolve the relationships between the hydraulic parameters T and S and the LB parameters. Transmissivity depends on the hydraulic conductivity, which is a function of permeability and fluid viscosity. Permeability is linked with the LB parameter $\mathbf{R}^*$ and the kinematic viscosity following Eq. (13); hence transmissivity (T) will be associated with $\mathbf{R}^*$, and dependence on τ, which controls kinematic viscosity, is also expected. The storage coefficient is a hydraulic parameter that controls the transient behavior of a confined aquifer, and τ is an LB parameter that controls the time evolution of particle dynamics. Hence, S is expected to be closely linked with τ. Based on testing of LB simulations against the analytical Theis solution described below for different values of $\mathbf{R}^*$ and τ, transmissivity T is associated with resistance field $\mathbf{R}^*$ as

$$T = \frac{\tau \mathbf{R}^{*-1}}{3}, \tag{24}$$

and the storage coefficient S was observed to be equal to the relaxation time τ.

The parameters used in the altered-velocity model of the transient ground water flow problem of Fig. 1 without source/sink are shown in Table 2. We arbitrarily select $\mathbf{R}^* = 1$ and $\tau_B = S = 0.96$, fix the length scale to 1 m = 1 lu and then use Eq. (23) to find the LB time corresponding to the real time. The transmissivity (T) of the aquifer is 0.32 lu^2/ts and the storage coefficient is equal to 0.96; hence, the hydraulic diffusivity ($\frac{T}{S}$) is $\frac{1}{3}$ lu^2/ts. Diffusion length as expressed in Eq. (23) is used to scale time steps between real units and lattice units. The results are shown in Fig. 2. The LB solution shows an excellent match with the analytical solution. This demonstrates the ability of the LB-based altered-velocity flow model to simulate an initial value problem from the groundwater discipline.

4. Transient groundwater flow problem with source/sink

Investigation of aquifer response to a pumping well is a common hydrological task and forms the basis of techniques for measuring the aquifer parameters, T and S. In the simplest case, the well is assumed to penetrate through the full thickness of aquifer and flow to the well is horizontal, so that equipotential (equal head) surfaces are vertical. Pumping a well causes a decrease in head/potential in the neighboring region as shown in Fig. 3 and develops cylindrical equipotential surfaces concentric on the well and the flow lines are radially inwards towards the pumping well. Head measurements from observation wells at different radii from the pumping well will be unique [21]. This is naturally a cylindrical co-ordinate problem but we solve it numerically in the Cartesian co-ordinate system. In the groundwater flow equation, an injection (source) or pumping (sink) well can be considered as a point source/sink and be represented by a node. The change in head (s), at any distance r, from the pumping well, compared to the original water level is called drawdown and drawdown plotted against time is called a drawdown curve as shown in Fig. 4. Any change in the head causes changes in storage for both confined and unconfined aquifers. The discharge, Q coming from the well must be equal to the aquifer yield, which is equal to product of storage coefficient S and rate at which head declines, integrated over the effective surface area of aquifer. The aquifer is assumed homogeneous and isotropic in all directions. Theis [22] presented an analytical solution to Eq. (3) for the following boundary and initial conditions

$$\begin{aligned} &h\,(r, 0) = h_0, \\ &h\,(\infty, t) = h_0, \\ &\lim_{r \to 0} \left[r \frac{\partial h}{\partial r} \right] = \frac{Q}{2\pi T}. \quad \forall t > 0 \end{aligned} \tag{25}$$

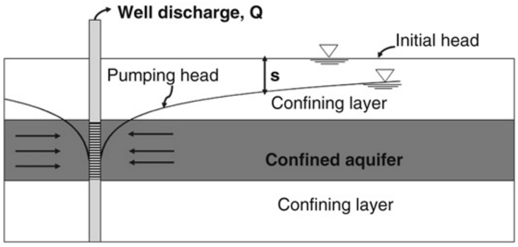

Fig. 3. Drawdown curve for pumping well in a confined aquifer.

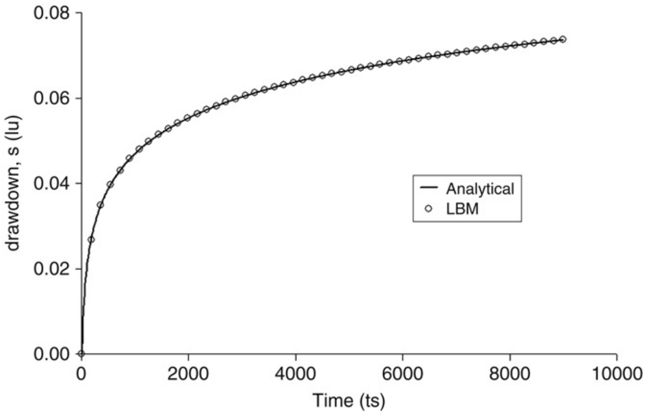

Fig. 4. Drawdown curve for pumping well in a confined aquifer.

h_0 is initial water table. The Theis solution for drawdown (s) is

$$s = \frac{Q}{4\pi T} \int_u^\infty \frac{e^{-z}}{z} dz \tag{26}$$

where $u = \frac{r^2 S}{4Tt}$. u determines the radius of the the cone of depression, transmissivity (T) controls the overall shape and extent of the cone, and storage coefficient (S) controls the volume (V) of the cone of depression in a confined aquifer [23]. The drawdown curve is different for confined and unconfined aquifers because for an unconfined aquifer, saturated thickness changes with pumping. The saturated thickness remains constant for confined aquifers. Hence, a confined aquifer is a simpler case to study and model compared to the unconfined aquifer.

The flux (q) is fixed at the sink node and the drawdown curve is observed in the neighboring region. We simulate a confined aquifer in a 500 lu $\times$500 lu domain with a uniform head (pressure) boundary on all four sides and a point sink node of strength equal to 0.051 lu/ts at the geometric center (250, 250) of the domain.

The initial drawdown was zero corresponding to an initial head represented by a uniform density of 1 mu/lu^3 over the whole domain. The drawdown (s) is observed at $r = 4$ lu from the sink node after every 15 ts. The boundaries are set far from the sink (well) node, so that the boundary conditions do not affect the drawdown curve [24]. In the analytical solution, drawdown in the infinite domain is due to pumping alone and the constant head boundary condition should not influence the transient change in head in the simulation. Hence, the drawdown in the simulations is observed only until the effect of pumping reaches the boundary, which gives the impression of an effectively infinite domain. The resistance tensor $\mathbf{R}^*$ and τ are set equal to 1, hence transmissivity is 1/3 lu^2/ts and the storage coefficient (S) is equal to 1.

The simulated drawdown is compared against the Theis solution [22] as shown in Fig. 4. The open circles are LB drawdown after every 180 ts and the solid line is the analytical solution. Hence, the LB-based altered-velocity flow solver can be used to simulate transient well problems for a confined aquifer.

The storage coefficient (S) has a strong influence on the drawdown curve. It indicates a combined effect of the elasticity of the rock and the compressibility of the water. In the LB model, the storage coefficient is equal to the relaxation time τ, hence S should always be greater than 0.5. This does not correspond to storage coefficients observed in the real world, which are typically 10^{-1}– 10^{-7}. Thus, we always need to use ξ (Eq. (23)) to scale hydraulic parameters and time. Results for different storage coefficients are shown in Fig. 5. The drawdown curve is drawn for a node at 4 lu from the pumping well for different values of storage coefficient (S) while keeping the hydraulic diffusivity (D) constant.

$\mathbf{R}^*$ is equal to 1, D equals $\frac{1}{3}$ lu^2/ts, and the pumping rate is equal to 0.051 lu/ts. The LB results are plotted after every 150 ts as shown by open circles and the analytical solution is shown by solid lines. There is some departure from the analytical

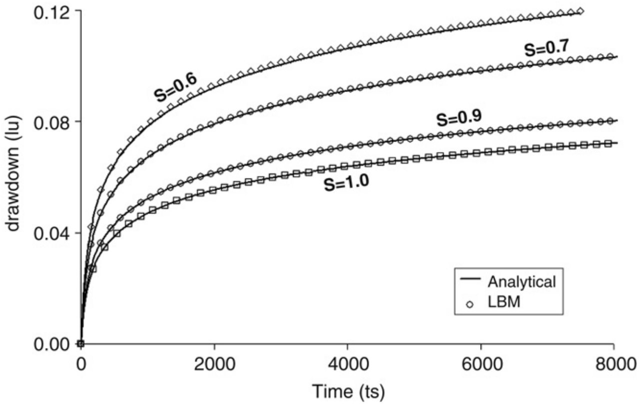

Fig. 5. Effect of storage coefficient (S) on the drawdown curve in a confined aquifer.

solution as S or τ gets closer to 0.5. In this model the hydraulic parameters T and S are treated separately unlike in our LB-based diffusion model without a source/sink where these parameters are lumped into one as a hydraulic diffusivity.

5. Conclusion

Two different kinds of LB-based models are used to solve transient groundwater flow problems. The analogy between the diffusion coefficient in the diffusion equation and hydraulic diffusivity in the groundwater flow equation is used to implement an LB-based diffusion model to solve the transient groundwater flow equation. The LB-based diffusion model is found to have limited applicability due to the inherent lumping of two hydraulic parameters (T and S) into one parameter hydraulic diffusivity (D) when there is no source/sink term. Our LB-based altered-velocity flow model is more flexible and able to solve transient problems with or without source/sink terms in its current form. The hydraulic parameters are treated separately in this model. T is linked with the resistance field ($\mathbf{R}^*$) and relaxation parameter τ. The Storage coefficient is found to be equal to τ. A non-dimensional number (ξ) is used to scale time and hydraulic diffusivity between LB units and real units. The results from LB-based models showed good agreement with available analytical solutions.

Acknowledgments

Anwar was supported by the Dissertation Year Fellowship (DYF) from the University Graduate School, Florida International University, Miami. We acknowledge support from the the United States Geological Survey and Center for Advanced Separation Technologies. This project was supported in part by the National Science Foundation under grant No 0440253.

References

[1] A. Cortis, B. Berkowitz, Anomalous transport in classical soil and sand columns, Soil. Sci. Soc. Amer. J. 68 (2004) 1539–1548.
[2] T.N. Narasimhan, Fourier's heat conduction equation: History, influence, and connections, Rev. Geophys. 37 (1) (1999) 151–172. doi:10.1029/1998RG900006.
[3] H.F. Wang, M.P. Anderson, Introduction to Groundwater Modeling: Finite Difference and Finite Element Methods, Academic Press, 1982, pp. 89.
[4] C. Pan, L.S. Luo, C.T. Miller, An evaluation of lattice Boltzmann schemes for porous medium flow simulation, Comput. & Fluids 35 (2006) 898–909.
[5] T. Inamuro, M. Yoshino, H. Inoue, R. Mizuno, F. Ogino, A lattice Boltzmann method for a binary miscible fluid mixture and its application to a heat-transfer problem, J. Comput. Phys. 179 (2002) 201–215.
[6] T. Inamuro, M. Yoshino, F. Ogino, Lattice Boltzmann simulation of flow in a three-dimensional porous structure, Internat. J. Numer. Methods Fluids 29 (1999) 737–748.
[7] Y. Qian, D. d'Humières, P. Lallemand, Lattice BGK models for Navier–Stokes equation, Europhys. Lett. 17 (1992) 479–484.
[8] I. Ginzburg, Equilibrium-type and link-type lattice Boltzmann models for generic advection and anisotropic-dispersion equation, Adv. Water Resour. 28 (11) (2005) 1171–1195.
[9] X. He, L.S. Luo, A priori derivation of the lattice Boltzmann equation, Phys. Rev. E 55 (6) (1997) R6333–R6336.
[10] B. ServánCamas, Salt water intrusion simulation in heterogeneous aquifer using lattice Boltzmann method, M.S. Thesis, Louisiana State University, Louisiana, 2007.
[11] M.A.A. Spaid, F.R. Phelan Jr., Lattice Boltzmann methods for modeling microscale flow in fibrous porous media, Phys. Fluids 9 (1997) 2468–2474.
[12] O. Dardis, J. McCloskey, Lattice Boltzmann scheme with real numbered solid density for the simulation of flow in porous media, Phys. Rev. E 57 (4) (1998) 4834–4837.
[13] D.M. Freed, Lattice-Boltzmann methods for macroscopic porous media modeling, Internat. J. Modern Phys. C 9 (1998) 1491–1503.
[14] Y. Gao, M.M. Sharma, A LGA model for fluid flow in heterogeneous porous media, Transp. Porous Media 17 (1994) 1–17.
[15] Q. Kang, D. Zhang, S. Chen, Unified lattice Boltzmann method for flow in multiscale porous media, Phys. Rev. E. 66 (2002) 056307-1–11.
[16] X. Shan, H. Chen, Lattice Boltzmann model for simulating flows with multiple phases and components, Phys. Rev. E 47 (3) (1993) 1815–1819.
[17] N.S. Martys, H. Chen, Simulation of multicomponent fluids in complex three-dimensional geometries by the lattice Boltzmann method, Phys. Rev. E. 53 (1) (1996) 743–750.
[18] H.R. Henry, Effects of dispersion on salt encroachment in coastal aquifers, US Geological Survey Water Supply Paper 1613-C (1964) C71–C84.
[19] E.G. Flekkøy, Lattice Bhatnagar–Gross–Krook models for miscible fluids, Phys. Rev. E 47 (6) (1993) 4247–4257.

[20] M.C. Sukop, D.T. Thorne Jr., Lattice Boltzmann Modeling: An Introduction for Geoscientists and Engineers, Springer, Heidelberg, Berlin, New York, 2006, pp. 172.
[21] J. Bear, Hydraulics of Groundwater, McGraw-Hill, New York, 1979.
[22] C.V. Theis, The relation between the lowering of the piezometric surface and the rate and duration of discharge of a well using ground-water storage, EOS 16 (2) (1935) 519–524.
[23] J.L. Osiensky, R.E. Williams, B. Williams, G. Johnson, Evaluation of drawdown curves derived from multiple well aquifer tests in heterogeneous environments, Mine Water Environ. 19 (1) (1992) 30–55.
[24] M.P. Anderson, W.W. Woessner, Applied Ground Water Modeling: Simulation of Flow and Advective Transport, Academic Press, 1992, pp. 237.
[25] Q. Zou, X. He, On pressure and velocity boundary conditions for the lattice Boltzmann BGK model, Phys. Fluids 9 (1997) 1591–1598.